Hesperetin improves diabetic coronary arterial vasomotor responsiveness by upregulating myocyte voltage-gated K^+ channels

YU LIU[1], LEI ZHANG[1], LINA DONG[1], QIYING SONG[1], PENGMEI GUO[1], YAN WANG[1], ZHAOYANG CHEN[2] and MINGSHENG ZHANG[1]

[1]Department of Pharmacology, Shanxi Medical University;
[2]Shanxi Key Laboratory of Experimental Animal Science and Animal Model of Human Disease, Laboratory Animal Center of Shanxi Medical University, Taiyuan, Shanxi 030001, P.R. China

Received May 18, 2019; Accepted March 3, 2020

DOI: 10.3892/etm.2020.8670

Abstract. Hesperetin (HSP) is a naturally occurring flavonoid. The present study aimed to investigate the potential vasomotor effects and mechanisms of HSP action on rat coronary arteries (RCAs) injured by diabetes or high glucose concentrations. HSP (100 mg/kg/day) was intragastrically administered to the rats for 8 weeks, which were rendered diabetic with a single intraperitoneal injection of 60 mg/kg streptozotocin (STZ). The vascular tone of RCAs was recorded using a wire myograph. The voltage-dependent K^+ (Kv) currents were examined using patch clamping. The expression of Kv channels (Kv1.2 and Kv1.5) was examined by western blot analysis and reverse transcription-quantitative PCR (RT-qPCR). Diabetes induced contractile hypersensitivity and vasodilator hyposensitivity in RCAs, both of which were attenuated by the chronic administration of HSP. Patch clamp data revealed that chronic HSP treatment reduced diabetes-induced suppression of Kv currents in the myocytes. Western blot and RT-qPCR analyses revealed that chronic HSP administration increased the expression of Kv1.2, but not Kv1.5, in the RCAs of diabetic rats compared with those from non-diabetic rats. *In vitro* analysis showed that co-incubation with HSP ameliorated high-glucose-induced suppression of Kv currents and Kv 1.2 protein expression in the myocytes. Taken together, the present study demonstrated that HSP alleviated RCA vasomotor dysfunction as a result of diabetes in rats by upregulating the expression of myocyte Kv channels.

Correspondence to: Dr Mingsheng Zhang or Dr Yu Liu, Department of Pharmacology, Shanxi Medical University, 56 Xinjiannanlu Street, Taiyuan, Shanxi 030001, P.R. China
E-mail: zmspharmacol@sina.com
E-mail: hitec@126.com

Key words: hesperetin, diabetes, coronary artery, voltage-dependent K^+ channel, high glucose

Introduction

Voltage-dependent potassium (Kv) channels have been previously demonstrated to serve an important role in canine and mouse coronary arterial vasomotor regulation (1,2). Streptozotocin (STZ)-induced diabetes weakened rat coronary arterial vasodilation responsiveness to the β-adrenoceptor agonist isoproterenol and the adenylyl cyclase activator forskolin, in addition to reducing Kv channel currents (1,2). Mechanistically, diabetes has been shown to downregulate the expression of Kv1.2 and Kv1.5 channels in arterial myocytes (3). High glucose concentrations have been previously revealed to weaken rat coronary arterial responsiveness to vasodilators isoproterenol and forskolin whilst augmenting arterial sensitivity to vasoconstrictors (4), in addition to inhibiting myocyte Kv currents in porcine coronary arteries, human internal mammary arteries, rat mesenteric and coronary arteries (5). Therefore, preserving the expression of Kv channels in myocytes may serve as a promising therapeutic strategy in protection against coronary arterial dysfunction under diabetic and hyperglycemic conditions.

Hesperetin (HSP) is one of the most abundant flavonoids found in citrus fruits (6). It was suggested that HSP may be of benefit in treating a number of ailments, including capillary fragility and hypertension (6). Higher intake of HSP in the daily diet was shown to be associated with a reduction in human mortality as a result of cardiovascular diseases, lung cancer and asthma (7). HSP contributes to the protective effects of orange juice to the vascular system (8,9). It was reported that HSP possesses antioxidant (10-12), hypolipidemic (13), anti-inflammatory (14), neuroprotective (15), cardioprotective (16), hypotensive (17) and anti-coagulation (18) properties, in addition to being effective in attenuating airway hypersensitivity (8,19). HSP has been demonstrated to exert vasculoprotective and anti-angiogenic effects in diabetic rats (20), in addition to inhibiting rat aortic smooth muscle cell proliferation (21). A previous study on isolated blood vessels showed that HSP treatment can induce rat aorta relaxation (22). However, the mechanism underlying HSP vasorelaxation currently remains controversial. Suggested

mechanisms include the enhancement of endothelial nitric oxide production (23), suppression of reactive oxygen species production (24), inhibition of phosphodiesterases (22) and activation of tetraethylammonium-sensitive K^+ channels (25). Review of these studies (19,22-25) suggests that the effects mediated by HSP are likely to involve multiple targets, where each mechanism may contribute additively to the eventual vasculoprotective effect downstream. A previous study showed that HSP relaxes rat coronary arteries (RCAs) isolated from healthy rats through, at least in part, an increase of myocyte Kv channel currents (26). Although accumulating evidence have indicated that HSP is promising in preventing and treating cardiovascular diseases (7-11,13), little is known about its effects on diabetic coronary arteries. Therefore, the present study was designed to examine the effects of HSP on the contraction-relaxation responsiveness of diabetic RCAs. In addition, the potential effects of HSP on Kv channel currents and the expression of Kv channels in rat coronary arterial smooth muscle cells (RCASMCs) following diabetes- or high glucose-induced injury were also investigated.

Materials and methods

Drugs and chemicals. HSP (analytical standard), L-glucose, collagenase F, collagenase H, dithiothreitol, acetylcholine chloride (Ach), 9,11-dideoxy-9a,11a-methanoepoxy prostaglandin $F_{2\alpha}$ (U46619), forskolin, 4-aminopyridine (4-AP), Na_2ATP, STZ, HEPES, potassium aspartate, sodium carboxmethylcellulose, DMEM, albumin and KCl were all purchased from Sigma-Aldrich; Merck KGaA. Papain was purchased from Worthington Biochemical Corporation. Penicillin G and streptomycin were purchased from Beijing SolarBio Science & Technology Co., Ltd.

Animals. The experimental protocols of the present study were approved by the Animal Care and Use Committee of Shanxi Medical University (approval no. 2018LL348; Taiyuan, China). The Animal Research: Reporting *In Vivo* Experiments guidelines were strictly adhered (27). A total of 48 male Sprague-Dawley rats (weight, 190-220 g; age, 7-8 weeks) were maintained at 24±2˚C, 50% humidity in a 12:12 h light/dark cycle. The rats had free access to a standard pellet diet and tap water.

General experimental protocol. The rats were fasted overnight and diabetes was induced by a single intraperitoneal injection of 60 mg/kg STZ dissolved in 0.1 M citrate buffer (pH 4.5). Age-matched non-diabetic rats were administered a single intraperitoneal injection of 0.1 M citrate buffer, which served as the non-diabetic control. One week after STZ administration, plasma glucose concentrations were measured using a glucometer. Rats with plasma glucose levels >250 mg/dl were designated as diabetic and randomly divided into 2 groups (n=16 rats per group): The diabetic control and the HSP-treated group (intragastric administration of HSP 100 mg/kg/day). Diabetic rats were treated with subcutaneous injection of ultralente insulin (Shanghai Fosun Pharmaceutical Group Co., Ltd.) 1-3 U/day to maintain moderate hyperglycemia to prevent ketoacidosis and severe weight loss (28). HSP dose and concentration were selected with reference to previous reports (20,24,26,29,30). HSP suspended in 0.1% sodium carboxymethyl cellulose was administered intragastrically once daily using a gavage needle with a volume of 2 ml/kg maintained throughout the experimental period for 8 weeks. In the same manner, 2 ml/kg vehicle (0.1% sodium carboxymethyl cellulose without HSP) was administered to the rats in the non-diabetic control and diabetic control groups. Body weight, food consumption and water intake were recorded once daily. By the end of 8 weeks following STZ administration, the rats were fasted overnight, anesthetized (intraperitoneal injection of 40 mg/kg sodium pentobarbital) and sacrificed by exsanguination from the left cephalic artery. Following sacrifice, the rat hearts were removed and the coronary arteries (inner diameter, 150-280 μm) were carefully isolated for myography, patch clamping, reverse transcription-quantitative PCR (RT-qPCR) and western blot analyses.

Measurement of isometric force. RCAs were cut into 2-mm long rings in 4˚C HEPES solution composed of the following: i) NaCl, 128 mM; ii) KCl, 4.7 mM; iii) $CaCl_2$, 2.5 mM; iv) $MgCl_2$, 1.2 mM; v) KH_2PO_4, 1.2 mM; vi) $NaHCO_3$ 10 mM; vii) HEPES 10 mM; and viii) D-glucose 11.0 mM; pH 7.4. The rings were mounted on a wire myograph (DMT-610 M; Danish Myo Technology A/S) using two 40 μm tungsten wires in a tissue chamber containing 5.0 ml HEPES solution bubbled with 95% O_2/5% CO_2 at 37˚C. The rings were stretched to a vascular tone equivalent to ~80 mmHg according to the manufacturer's protocols and equilibrated for 2 h. Following equilibration, the rings were stimulated with 60 mM KCl for 20 min repeatedly. The ring was then allowed to recover for 40 min after each stimulation. When the contraction responses become reproducible, concentration-contraction curves or concentration-relaxation curves were constructed. In experiments of KCl-induced contraction, equivalent concentrations of NaCl were replaced with KCl to exclude the effect of osmolality.

The concentration-contraction curves of KCl (20,28,39,55 and 77 mM) were constructed through the cumulative addition of the KCl HEPES solution into the chamber. In a similar manner, curves for U46619 (10^{-8}-10^{-6} M) were also constructed. The contraction response to each concentration of an agonist was allowed to reach a relative tone plateau. Vasodilator concentration-relaxation curves for acetylcholine ($3x10^{-8}$-10^{-5} M) and forskolin (10^{-8}-$3x10^{-6}$ M) were constructed by the cumulative addition of vasodilator to the chamber when the contraction response to 60 mM KCl or 1 μM U46619 was observed to be sustained. Relaxations were expressed as the percentage of the contraction induced by 60 mM KCl or 1 μM U46619, respectively, prior to treatment with the vasodilators.

Electrophysiological measurements. For single RCASMC isolation, RCAs were dissected in 0.1 mM $CaCl_2$ HEPES solution containing 0.5 mg/ml papain, 1 mg/ml dithiothreitol and 1 mg/ml albumin, which was then incubated for 25 min at 37˚C. Subsequently, the arteries were transferred to the same solution deprived of Ca^{2+} and incubated for 10 min at 37˚C. Single cells were dispersed mechanically using a Pasteur pipette. Isolated RCASMCs were used immediately for electrophysiological recording or stored in Ca^{2+}-free 4˚C HEPES solution for later use within 8 h of isolation.

Table I. Effects of chronic HSP treatment on body weight and plasma levels of glucose.

Groups	n	Body weight (g)	Plasma glucose (mM)
Non-diabetic	16	328.55±9.91	5.94±0.60
Diabetic	13	219.19±10.32[a]	29.77±2.73[a]
Diabetic+HSP	14	264.08±9.40[b]	20.54±2.34[b]

[a]P<0.05 vs. Non-diabetic and [b]P<0.05 vs. Diabetic. HSP, hesperetin.

Single RCASMCs were plated onto the glass bottom dishes and visualized using an inverted microscope (magnification x400; ECLIPSE TE2000-S; Nikon Corporation). Cells were allowed to settle for 30 min and were gently washed using HEPES solution to remove debris. Electrophysiological responses were only recorded in cells that are firmly adhered to the bottom surface of the chamber and morphologically characteristic of arterial smooth muscle cells (ASMCs) with clearly defined and visible cell membranes. All electrophysiological experiments were performed in an air-conditioned room at ~25˚C. Patch electrodes were pulled from borosilicate glass capillary tubing (outside diameter, 1.5 mm; inside diameter, 0.84 mm; Vitalsense Scientific Instruments Co., Ltd.) using a micropipette puller (PP-830; Narishige Group) and polished on a microforge (MF-830; Narishige Group). The electrodes had resistances of 3-5 MΩ when filled with a pipette solution as undermentioned. Whole-cell voltage clamp was performed using an Axopatch 200B amplifier (Axon Instruments), a 32-bit data acquisition system (Digidata1440A, Molecular Devices, LLC.) and the pClampex software 10.4 (Molecular Devices, LLC.). Pipette offset, whole-cell capacitance and series resistance (to 80%, bandwidth >5 kHz) were electronically compensated. The average access resistance was 3-5 MΩ and the cell capacitance was 7-15 pF. Current traces were filtered at 1 kHz with a low-pass 4-pole Bessel filter in the clamp amplifier, subjected to P/4 leak subtraction and digitized at 5 kHz before being stored on the computer hard drive for subsequent analysis using pClampex 10.4.

Cells were perfused with a Ca^{2+}-free HEPES bath solution. The pipette was filled with a Ca^{2+}-free HEPES solution consisting of the following: i) KCl, 110 mM; ii) $MgCl_2$, 1.2 mM; iii) Na_2ATP, 5 mM; iv) EGTA, 10 mM; and v) HEPES, 10 mM; with the pH adjusted to 7.3 using KOH. Under these conditions, ATP-sensitive K^+ channel (K_{ATP}) currents and Ca^{2+}-activated K^+ channel (K_{Ca}) currents were minimized by the inclusion of high concentrations of ATP and EGTA in the pipette solution (31). The remainder of the K^+ currents were markedly attenuated by the Kv channel blocker 4-aminopyridine (4-AP; 3 mM), which were considered as K^+ currents mediated by Kv channels (31). Cells were held at holding potentials of -60 mV and subsequently subjected to step depolarizations to +80 mV in 10 mV increments at 500 msec each.

RT-qPCR. RCAs freshly isolated from diabetic or non-diabetic rats were used for RT-qPCR analysis. RT-qPCR was used to detect transcript levels as previously described (32-34). SV Total RNA Isolation System (Promega Corporation) was used to isolate total RNA from the RCAs in accordance to the manufacturer's protocol. A microplate reader (BioTek Instruments, Inc.) was used to measure the concentration and purity of the RNA samples. A total of 1 μg RNA was added into the reaction system (PrimeScript™ RT reagent kit with gDNA Eraser; Takara Bio, Inc.) comprising of 2 μl 5X gDNA Eraser Buffer, 1 μl gDNA Eraser and appropriate volumes DEPC-treated water to remove genomic DNA. The mixture was then incubated for 2 min at 42˚C. Total RNA was converted into cDNA in a 20 μl PCR reaction system with 10 μl reaction system from the previous step, 1 μl PrimeScript RT Enzyme Mix I, 1 μl RT Primer Mix, 4 μl 5X Primer Script Buffer 2, 4 μl RNase Free dH_2O (PrimeScript™ RT reagent kit with gDNA Eraser; Takara Bio, Inc.). C1000 Touch™ Thermal cyclers (Bio-Rad Laboratories, Inc.) were used to perform RT with the following heat cycle: 37˚C for 15 min and 85˚C for 5 sec. A total of 2 μl cDNA was amplified in a 23 μl reaction system containing 12.5 μl SYBR® Premix Ex Taq™ (Takara Bio, Inc.), 8.5 μl DEPC-treated water, 1 μl forward primer (10 μM) and 1 μl reverse primer (10 μM). The following thermocycling conditions were used for the PCR: Initial denaturation at 95˚C for 30 sec; followed by 40 cycles of 95˚C for 5 sec and 60˚C for 30 sec. The melting curve included an increase from 65˚C to 95˚C for 5 sec. The following primer pairs were used for the qPCR: Kv1.2 forward, 5'-TGTCTATCACCCAGGAACATGGAG-3' and reverse, 5'-GAGCTTGGGTCTGAAGCCTTTG-3'; Kv1.5 forward, 5'-CCTCCGACGTCTGGACTCAATAA-3' and reverse, 5'-CCTCATCCTCAGCAGATAGCCTTC-3' and GAPDH forward, 5'-GGCACAGTCAAGGCTGAGAATG-3' and reverse, 5'-ATGGTGGTGAAGACGCCAGTA-3' (Takara Bio, Inc.). Relative gene expression was calculated using the $2^{-\Delta\Delta Cq}$ method (35).

Western blotting. Total protein was extracted from RCA samples using RIPA buffer mixed with PMSF (Beijing SolarBio Science & Technology Co., Ltd.), protease inhibitor cocktail (Beyotime Institute of Biotechnology) and phosphatase inhibitor (Boster Biological Technology) at 4˚C for 30 min. The homogenate was cleared of debris by centrifugation at 13,000 x g at 4˚C for 20 min. Protein concentration was determined using a Bio-Rad protein assay (Bio-Rad Laboratories, Inc.) using BSA as a standard. Total protein (24 μg) was separated in a 10% Tris-HCl polyacrylamide gel and transferred onto nitrocellulose blotting membranes. The membranes were blocked in 5% non-fat milk containing TBS-0.02% Tween-20 (TBS-T) at room temperature for 2 h. The membranes were then incubated with polyclonal antibodies against Kv1.2 (1:400; cat. no. APC-004; Alomone Labs), Kv1.5 (1:400; cat. no. APC-010; Alomone Labs) or β-actin (1:4,000; cat. no. D110001-0100; Sangon Biotech Co., Ltd.) overnight at 4˚C. Following incubation with primary antibodies, the membranes were washed three times with TBS-T for 10 min and incubated with horseradish peroxidase-conjugated secondary antibodies (1:5,000; cat. no. ZB2301; Origene technologies, Inc.) for 1 h at room temperature. After the membrane was washed three times at 10 min intervals in TBS-T, the bound antibodies were detected with an ECL reagent using a ChemiDoc XRS chemiluminescence detection system (Bio-Rad Laboratories, Inc.). The levels of β-actin were used as internal controls for

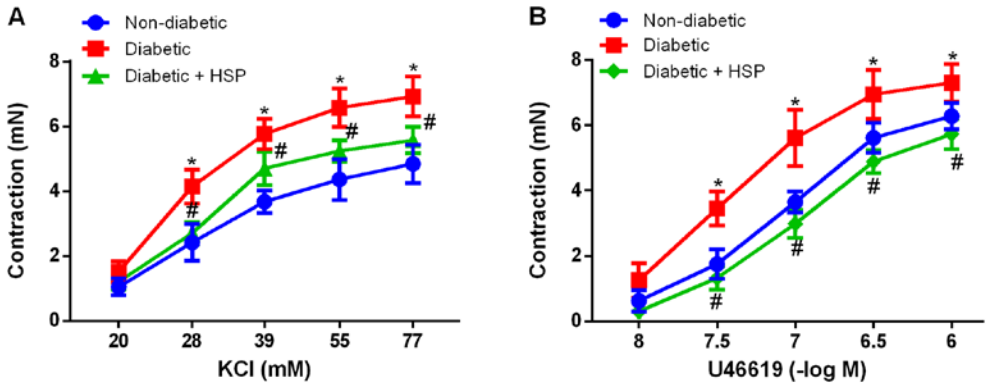

Figure 1. Chronic administration of HSP attenuates the enhanced contractility in diabetic RCAs. Cumulative concentration-contraction curves of (A) KCl or (B) U46619 were constructed in coronary arteries isolated from rats 8 weeks after streptozotocin injection. Each ring was isolated from a different rat. Results are presented as force increases (mN). n=6-8. *P<0.05 vs. Non-diabetic and #P<0.05 vs. Diabetic. HSP, hesperetin; U46619, 9,11-dideoxy-9a,11a-methanoepoxy prostaglandin $F_{2\alpha}$.

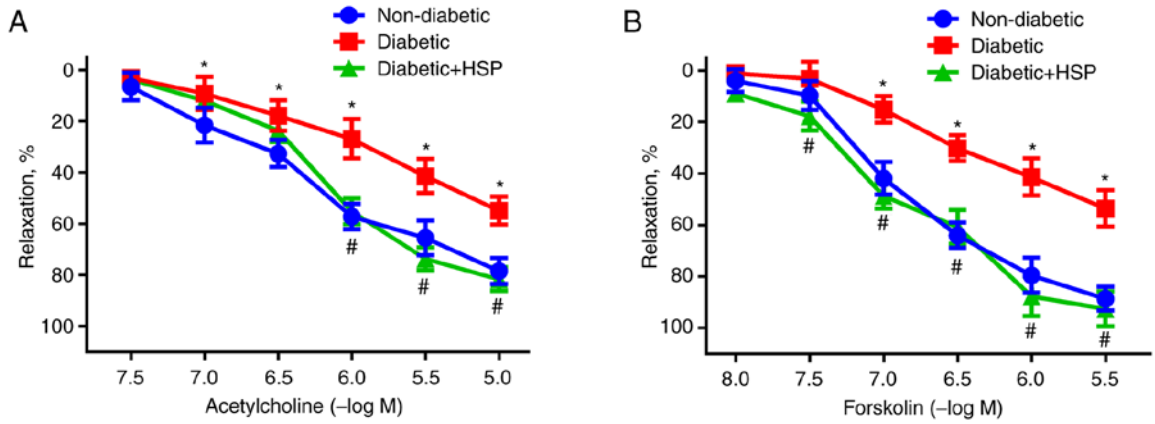

Figure 2. Chronic administration of HSP ameliorated the reduced relaxant responsiveness in diabetic RCAs. Relaxations in response to (A) acetylcholine and (B) forskolin were expressed as percentages of the precontraction induced by 1 μM U46619. Each ring was isolated from a different rat. n=6-8. *P<0.05 vs. Non-diabetic and #P<0.05 vs. Diabetic. HSP, hesperetin; U46619, 9,11-dideoxy-9a,11a-methanoepoxy prostaglandin $F_{2\alpha}$.

sample loading. Protein levels were quantified using Image Lab software (5.2.1, Bio-Rad Laboratories, Inc.).

Acute incubation experiment. As previously described (36), RCAs isolated from normal rats were incubated with various concentrations of glucose for 8 h in the presence or the absence of HSP prior to RCASMC isolation for patch clamping analysis, RT-qPCR and western blot assays. The incubation was performed in DMEM with 10% FBS (Sangon Biotech Co., Ltd.), 100 U/ml penicillin G and 100 mg/ml streptomycin for 24 h at 37˚C. DMEM was supplemented with either 5.5 mM D-glucose [normal glucose (NG); Tianjin Damao Chemical Reagent Factory], 44 mM D-glucose (high glucose, HG) or 5.5 mM D-glucose + 38.5 mM L-glucose (HLG). HLG served as an osmotic control as L-glucose cannot be metabolized. All media were filtered (0.2-mm filter) before use.

Statistical analysis. All data are expressed as the mean ± SD. Statistical analysis was performed using ANOVA followed by Tukey's multiple comparisons test using SPSS version 13 (SPSS, Inc.). P<0.05 was considered to indicate a statistically significant difference. 'n' represents the number of vascular rings or cells isolated from separate rats. The maximal contraction (E_{max}), the values of EC_{50} (vasoconstrictor concentration producing 50% of the maximal contraction) and RC_{50} (vasodilator concentration inducing 50% relaxation on the precontraction) were calculated by non-linear regression using GraphPad Prism version 6.0 (GraphPad Software, Inc.).

Results

Chronic HSP attenuates diabetes-induced losses in body weight and elevations in plasma glucose levels. At the end of 8 weeks after STZ injection, the body weight of vehicle-treated diabetic rats was found to be significantly lower (219.19±10.32 g vs. 328.55±9.91 g; P<0.05) whilst the plasma glucose concentration was significantly higher (29.77±2.73 mM vs. 5.94±0.60 mM; P<0.05) compared with those in non-diabetic rats (Table I). Compared with vehicle-treated diabetic rats, those treated with HSP exhibited significantly higher body weights (264.08±9.40 g vs. 219.19±10.32; P<0.05) and lower plasma glucose levels (20.54±2.34 mM vs. 29.77±2.73 mM; P<0.05; Table I).

Chronic HSP treatment reverses contractile hypersensitivity in diabetic RCAs. Both KCl (20-77 mM) and U46619

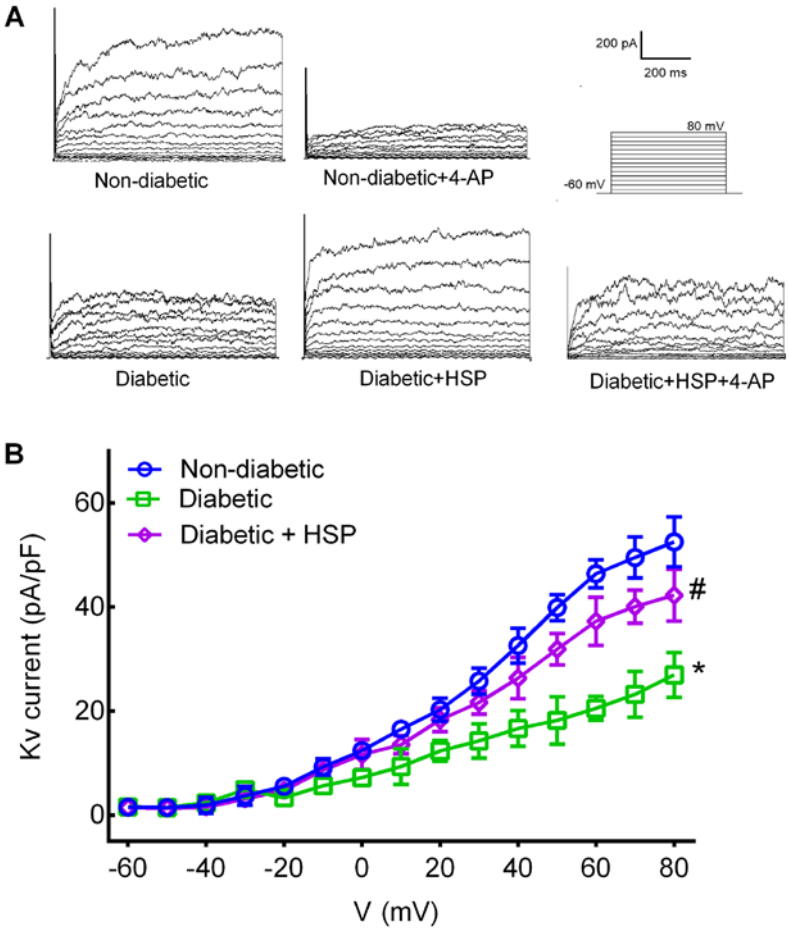

Figure 3. Chronic administration of HSP augmented Kv currents in diabetic RCASMCs. (A) Representative original recordings of the outward K^+ currents in response to a series of depolarizing pulses (from -60 to +80 mV in 10-mV increments, 500 ms duration) in myocytes. (B) Collective current-voltage curves of Kv currents recorded from myocytes isolated from the three experimental groups. Each cell was freshly isolated from a different rat. Data are expressed as Kv current density (mean ± SD). n=6-9. *P<0.05 vs. RCASMCs, rat coronary artery smooth muscle cells; Non-diabetic and #P<0.05 vs. Diabetic. HSP, hesperetin; 4-AP; 4-aminopyridine; Kv, voltage-dependent K^+ current; V, voltage.

(10^{-8}-10^{-6} M) application resulted in RCA contraction in a dose-dependent manner in all three experimental groups (Fig. 1). In the non-diabetic group, the E_{max} values for KCl and U46619 were calculated to be 4.85±0.59 and 6.28±0.41 mN, respectively (Fig. 1). By contrast, diabetic rats exhibited significantly higher E_{max} values, 6.93±0.61 mN for KCl (P<0.05) and 7.31±0.57 mN for U46619 (P<0.05). Compared with the vehicle-treated diabetic group, HSP treatment significantly decreased E_{max} for KCl to 5.58±0.34 mN (P<0.05; Fig 1A) and E_{max} for U46619 to 5.73±0.47 mN (P<0.05; Fig 1B).

Chronic HSP treatment restores relaxant responsiveness in diabetic RCAs. Ach (Fig. 2A) and forskolin (Fig. 2B) induced dose-dependent relaxations in all RCA rings pre-contracted with 1 μM U46619. The degree of relaxation as a result of Ach or forskolin treatment was observed to be significantly lower in the vehicle-treated diabetic group compared with that in the non-diabetic group (P<0.05). By contrast, Ach and forskolin treatment resulted in significantly higher degrees of relaxation in the HSP-treated diabetic group compared with those in the vehicle-treated diabetic group (P<0.05).

Chronic HSP treatment increases Kv currents in diabetic RCASMCs. Under the present experimental conditions, outward K^+ currents mediated through K_{ATP} and K_{Ca} channels were minimized by the inclusion of high concentrations of ATP and EGTA in the pipette solution. The remaining outward K^+ currents were found to be markedly attenuated by the Kv channel blocker 4-AP (3 mM), which were considered to be currents mediated by Kv channels (31). At a testing potential of +80 mV, the Kv current densities were significantly reduced (26.96±4.33 pA/pF vs. 52.51±4.86 pA/pF, P<0.05) in the vehicle-treated diabetic group, compared with those in the non-diabetic group (Fig. 3). By contrast, the Kv current densities were found to be significantly increased (42.27±5.02 pA/pF vs. 26.96±4.33 pA/pF, P<0.05) in the HSP-treated diabetic group compared with those in the vehicle-treated diabetic group.

Chronic HSP treatment increases the expression of Kv1.2 channels in diabetic RCASMCs. To explore the possible involvement of HSP treatment on the expression of Kv1.2 and Kv1.5 channel subtypes, both of which are important for coronary vasomotor function (37,38), Kv1.2 and Kv1.5 mRNA and protein expression were measured in RCASMCs by RT-qPCR and western blot analysis. The expression of Kv1.2, but not Kv1.5 channels, was significantly lower in diabetic rats compared with that in non-diabetic rats (Fig. 4). Diabetic rats treated with HSP exhibited significantly increased Kv1.2

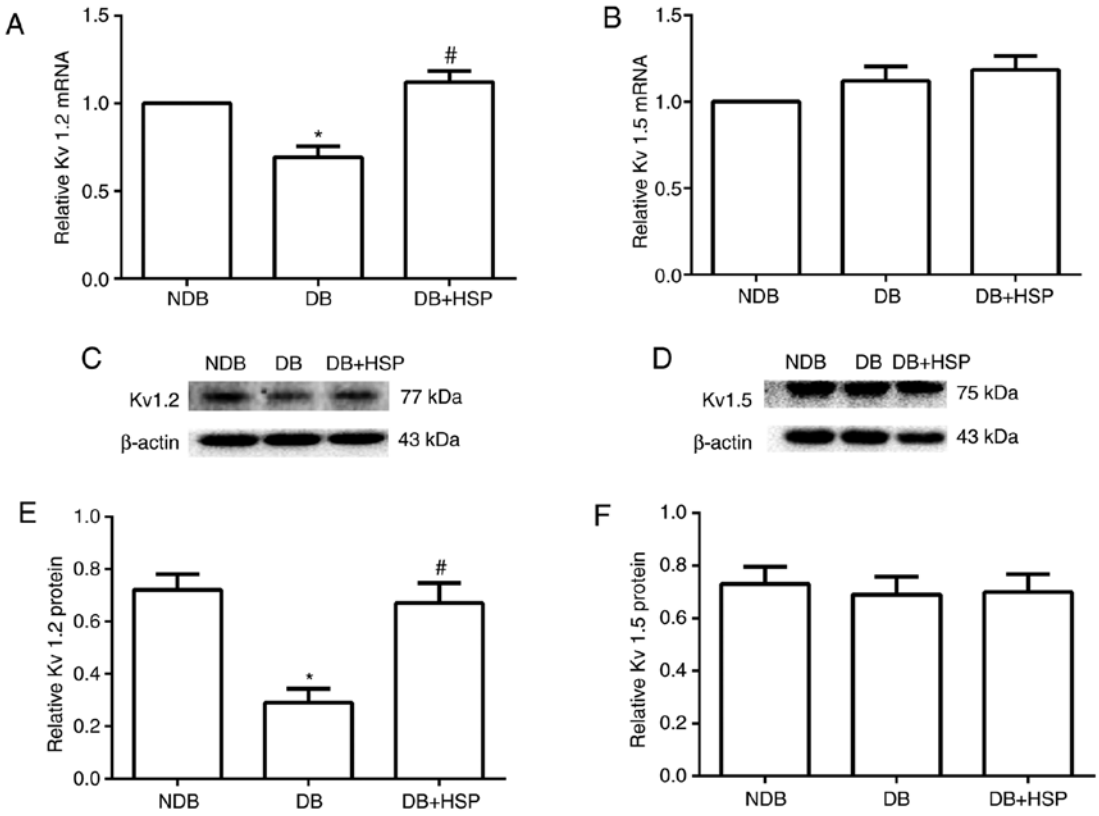

Figure 4. Chronic administration of HSP upregulated mRNA and protein expression of Kv1.2 in diabetic RCASMCs. The mRNA levels of myocyte (A) Kv 1.2 and (B) Kv 1.5 channels in the three experimental groups, which were expressed as the percentage relative to NDB. Representative western blot images showing (C) Kv1.2 and (D) Kv1.5 channel protein expression. The β-actin-normalized densitometric values of (E) Kv1.2 and (F) Kv1.5 channel protein expression in rat coronary arteries. Each value was presented as a mean ± SD from 6 measurements of pooled samples from 6-12 animals. *P<0.05 vs. NDB and #P<0.05 vs. DB. RCASMCs, rat coronary artery smooth muscle cells; Kv, voltage-dependent K^+ channels; HSP, hesperetin; NDB, non-diabetic control; DB, vehicle-treated diabetic control; DB + HSP, vehicle-treated diabetic control treated with hesperetin.

expression on both mRNA and protein levels compared with those of vehicle-treated diabetic rats (Fig. 4).

Acute application of HSP attenuates the suppression of Kv currents by high glucose in RCASMCs. Incubation of RCASMCs with 44 mM glucose (HG) for 8 h suppressed the Kv current density at a test potential of +80 mV compared with that in the normal control (NG) (36.48±4.62 pA/pF vs. 56.17±3.85, P<0.05), but not osmotic elevation with L-glucose (HLG, 56.83±5.01 pA/pF). Co-incubation with 30 μM HSP significantly attenuated high glucose-induced suppression of the Kv current (47.47±3.68 pA/pF, P<0.05), whilst 100 μM HSP treatment significantly reversed the suppression (61.25±5.51 pA/pF, P<0.05; Fig. 5).

Acute application of HSP attenuates high-glucose-induced downregulation of Kv1.2 expression in RCASMCs. Incubation of RCASMCs for 8 h with 44 mM glucose (HG) reduced Kv1.2 protein expression by 41.93% compared with NG, which was significantly reversed by co-incubation with 100 μM HSP (Fig. 6). Treatment with 30 μM HSP also increased Kv1.2 protein expression, but no statistical significance was observed compared with that in HG (Fig. 6).

Discussion

The present study investigated the effects of intragastric HSP administration on coronary arterial vasomotor function in rats with STZ-induced diabetes. The main findings of the present study were as follows: i) Chronic HSP administration improved contraction-relaxation responsiveness of diabetic RCAs; ii) chronic HSP administration augmented Kv channel currents and upregulated the expression of Kv1.2 channels in diabetic RCASMCs; and iii) acute incubation with HSP counteracted both the reduction of Kv channel currents and downregulation of Kv1.2 expression induced by high glucose in RCASMCs.

The STZ-induced diabetic rat model is a widely accepted animal model of diabetes as the rats typically exhibit characteristic symptoms of diabetes, including hyperglycemia, glucose intolerance, body weight loss and vascular dysfunction (39). In the present study, the diabetic rats exhibited significant decreases in body weight and higher glucose levels compared with non-diabetic rats. Chronic administration of HSP (100 mg/kg per day for 8 weeks) attenuated the diabetes-induced reductions in body weight loss and hyperglycemia. These effects could be due to the stimulation of glucose uptake by peripheral tissues, antioxidation, renoprotection and protective effects on pancreatic islet β-cells, based on previous reports (40,41). Compared with RCAs from non-diabetic rats, RCAs from diabetic rats exhibited increased sensitivity to vasoconstrictors KCl and U46619 whilst exhibiting opposite effects to vasodilators Ach and forskolin. Ach is an endothelium-dependent vasodilator whereas forskolin is an endothelium-independent

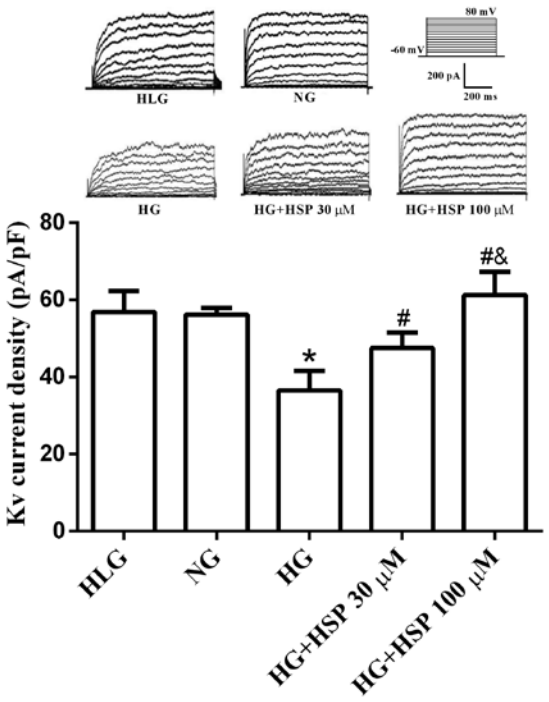

Figure 5. Co-incubation of RCASMCs with HSP attenuated the suppression of Kv currents in myocytes by HG. Data are presented as Kv current density in response to test potential of +80 mV. Each cell was isolated from a different rat. n=6-9. *P<0.05 vs. NG; #P<0.05 vs. HG and &P<0.05 vs. HG + HSP 30 μM. RCASMCs, rat coronary artery smooth muscle cells; HSP, hesperetin; HLG, osmotic control; NG, normal glucose; HG, high glucose; Kv, voltage-dependent K^+ current.

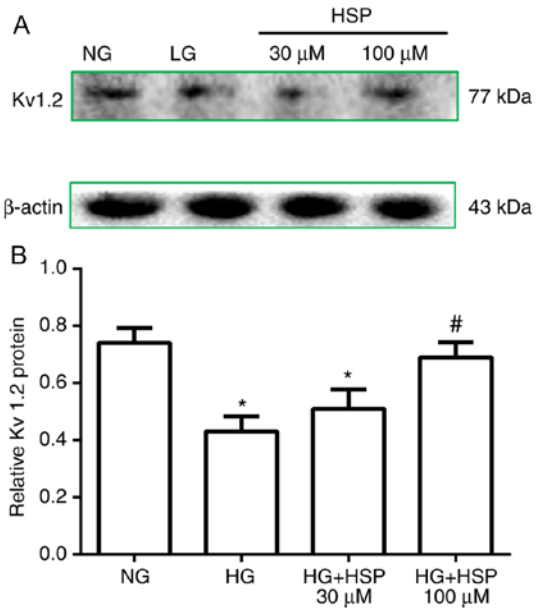

Figure 6. Co-incubation of RCASMCs with HSP reversed high glucose-induced reductions in Kv1.2 channel expression. (A) Representative western blotting images of Kv1.2 channel protein expression. (B) β-actin-normalized densitometric values of Kv1.2 channel protein expression in RCASMCs. Each value was presented as a mean ± SD from 6 measurements of pooled samples from 6-12 animals. *P<0.05 vs. NG and #P<0.05 vs. HG. RCASMCs, rat coronary artery smooth muscle cells; HSP, hesperetin; HLG, osmotic control; NG, normal glucose; HG, high glucose.

vasodilator, which induces vasodilation through adenylyl cyclase activation (42). These data suggest that both endothelium-dependent and endothelium-independent vasodilation pathways were impaired in diabetic rats, consistent with previous findings (43-47).

The present study demonstrated that chronic HSP not only attenuated diabetes-induced RCA hypersensitivity to KCl and U46619, but also restored the sensitivity of RCAs to vasodilators. These results implicate at the extension of the vasospasmolytic effects of HSP to diabetic RCAs. The observation that HSP restored responsiveness to both endothelium-dependent and -independent vasodilators suggested that in addition to possible effects on the endothelium, HSP also may exert direct effects on RCASMCs. This is consistent with a previous finding that HSP inhibited the myocyte voltage-dependent Ca^{2+} channels and increased the myocyte Kv channel activity (26).

K^+ channels are pivotal in the maintenance of cell membrane potential and regulation of vascular tone in coronary arteries (48). The activation of K^+ channels leads to K^+ efflux, membrane hyperpolarization, reducing Ca^{2+} influx into the cell and resistance to vascular myocyte contraction (49). Among a number of K^+ channel families, Kv channels are significant in the regulation of coronary arterial resistance (50-53). Both diabetes (1) and high glucose (5) have been previously demonstrated to reduce Kv channel currents and downregulated the expression of Kv 1.2 channels in RCASMCs. Therefore, it was hypothesized in the present study that improvement of Kv channel activity may be involved in the beneficial effects of HSP on RCAs of diabetic rats.

Although it was suggested that a number of mechanisms are involved in the vasorelaxant effects of HSP (22-25), none could adequately explain the vascular effects of HSP. A recent *in vitro* study demonstrated that HSP relaxed coronary arteries isolated from normal rats by increasing Kv currents and inhibiting Ca^{2+} influx in ASMCs (26). To explore the mechanism underlying the protective effects of HSP on RCAs from diabetic rats, Kv channel function was evaluated using the patch clamp technique. Kv currents were found to be increased in chronically HSP-treated diabetic rats compared with those in vehicle-treated diabetic rats. These results suggest that recovery of Kv function in RCASMCs may underlie the improvements in diabetic coronary arteries in response to HSP. To substantiate this, Kv channel expression was measured in RCAs from diabetic rats and in RCAs pre-incubated with high glucose. Diabetic induction was found to reduce the expression of Kv1.2 channels, but not Kv1.5. Chronic HSP administration increased the expression of Kv1.2, but not Kv1.5, in diabetic rats. Since elevated glucose is the main cause of diabetes-induced damage to the vasculature (54), the present study also investigated the *in vitro* effects of high glucose on the physiology of Kv channels. It was found that high glucose reduced Kv currents and downregulated Kv1.2 protein expression, both of which were reversed by co-incubation with HSP.

HSP depressed depolarization-induced contractions in both non-diabetic and diabetic RCAs, suggesting that apart from its potential effects on Kv channels, other

mechanisms may be involved in its protective effects (22-26). The molecular signaling mechanisms underlying vascular contraction-relaxation and the regulation of Kv channel function are complex (55-57). The effects of HSP on the expression profiles of the Kv1 channel subunits and associated signaling pathways remain to be clarified. To the best of our knowledge, the present study was the first to report the beneficial effects of HSP on diabetic coronary arteries via the upregulation of myocyte Kv channels.

In conclusion, the present study demonstrated that HSP restored the contraction-relaxation responsiveness of diabetic RCAs, augmented Kv currents and upregulated the expression of Kv1.2 channels in RCASMCs of diabetic rats or in RCASMCs exposed to high glucose. These results suggested that HSP may be a promising therapeutic agent for the treatment of coronary arterial dysfunction as a result of diabetes.

Acknowledgements

Not applicable.

Funding

The present study was supported by the National Natural Science Foundation of China (grant nos. NSFC81603111 and NSFC 81773738), The Fund for Shanxi Key Subjects Construction and The Fund for Shanxi 1331 Project Key Subjects Construction (grant no. XK200708).

Availability of data and materials

The datasets used and/or analyzed during the current study are available from the corresponding author on reasonable request.

Authors' contributions

YL and MZ designed the experiments, analyzed the data, prepared the figures and wrote the manuscript. YL, LD, QS, PG, YW and ZC performed the chronic experiments and myograph study. LZ, LD and PG performed the patch clamp technique; QS and YW performed RT-qPCR and western blot analysis. All authors contributed to drafting the manuscript. All authors read and approved the final manuscript.

Ethics approval and consent to participate

The authors declare that all protocols and procedures described in this animal study were approved by the Animal Ethics Committee of Shanxi Medical University (approval no. 2018LL348; Taiyuan, China). No human body materials and data were used in the present study.

Patient consent for publication

Not applicable.

Competing interests

The authors declare that they have no competing interests.

References

1. Chai Q, Liu Z and Chen L: Effects of streptozotocin-induced diabetes on Kv channels in rat small coronary smooth muscle cells. Chin J Physiol 48: 57-63, 2005.
2. Bubolz AH, Li H, Wu Q and Liu Y: Enhanced oxidative stress impairs cAMP-mediated dilation by reducing Kv channel function in small coronary arteries of diabetic rats. Am J Physiol Heart Circ Physiol 289: H1873-H1880, 2005.
3. Chai Q, Xu X, Jia Q, Dong Q, Liu Z, Zhang W and Chen L: Molecular basis of dysfunctional Kv channels in small coronary artery smooth muscle cells of streptozotocin-induced diabetic rats. Chin J Physiol 50: 171-177, 2007.
4. Jackson R, Brennan S, Fielding P, Sims MW, Challiss RA, Adlam D, Squire IB and Rainbow RD: Distinct and complementary roles for alpha and beta isoenzymes of PKC in mediating vasoconstrictor responses to acutely elevated glucose. Br J Pharmacol 173: 870-887, 2016.
5. Liu Y, Terata K, Rusch NJ and Gutterman DD: High glucose impairs voltage-gated K(+) channel current in rat small coronary arteries. Circ Res 89: 146-152, 2001.
6. Garg A, Garg S, Zaneveld LJ and Singla AK: Chemistry and pharmacology of the citrus bioflavonoid hesperidin. Phytother Res 15: 655-669, 2001.
7. Knekt P, Kumpulainen J, Järvinen R, Rissanen H, Heliövaara M, Reunanen A, Hakulinen T and Aromaa A: Flavonoid intake and risk of chronic diseases. Am J Clin Nutr 76: 560-568, 2002.
8. Morand C, Dubray C, Milenkovic D, Lioger D, Martin JF, Scalbert A and Mazur A: Hesperidin contributes to the vascular protective effects of orange juice: A randomized crossover study in healthy volunteers. Am J Clin Nutr 93: 73-80, 2011.
9. Rendeiro C, Dong H, Saunders C, Harkness L, Blaze M, Hou Y, Belanger RL, Corona G, Lovegrove JA and Spencer JPE: Flavanone-rich citrus beverages counteract the transient decline in postprandial endothelial function in humans: A randomised, controlled, double-masked, cross-over intervention study. Br J Nutr 116: 1999-2010, 2016.
10. Choi EJ: Antioxidative effects of hesperetin against 7,12-dimethylbenz(a)anthracene-induced oxidative stress in mice. Life Sci 82: 1059-1064, 2008.
11. Kim JY, Jung KJ, Choi JS and Chung HY: Hesperetin: A potent antioxidant against peroxynitrite. Free Radic Res 38: 761-769, 2004.
12. Pollard SE, Whiteman M and Spencer JP: Modulation of peroxynitrite-induced fibroblast injury by hesperetin: A role for intracellular scavenging and modulation of ERK signalling. Biochem Biophy Res Commun 347: 916-923, 2006.
13. Morin B, Nichols LA, Zalasky KM, Davis JW, Manthey JA and Holland LJ: The citrus flavonoids hesperetin and nobiletin differentially regulate low density lipoprotein receptor gene transcription in HepG2 liver cells. J Nutr 138: 1274-1281, 2008.
14. Hirata A, Murakami Y, Shoji M, Kadoma Y and Fujisawa S: Kinetics of radical-scavenging activity of hesperetin and hesperidin and their inhibitory activity on COX-2 expression. Anticancer Res 25: 3367-3374, 2005.
15. Huang SM, Tsai SY, Lin JA, Wu CH and Yen GC: Cytoprotective effects of hesperetin and hesperidin against amyloid beta-induced impairment of glucose transport through downregulation of neuronal autophagy. Mol Nutr Food Res 56: 601-609, 2012.
16. Trivedi PP, Kushwaha S, Tripathi DN and Jena GB: Cardioprotective effects of hesperetin against doxorubicin-induced oxidative stress and DNA damage in rat. Cardiovasc Toxicol 11: 215-225, 2011.
17. Yamamoto M, Suzuki A and Hase T: Short-Term effects of glucosyl hesperidin and hesperetin on blood pressure and vascular endothelial function in spontaneously hypertensive rats. J Nutr Sci Vitaminol (Tokyo) 54: 95-98, 2008.
18. Jin YR, Han XH, Zhang YH, Lee JJ, Lim Y, Chung JH and Yun YP: Antiplatelet activity of hesperetin, a bioflavonoid, is mainly mediated by inhibition of PLC-gamma2 phosphorylation and cyclooxygenase-1 activity. Atherosclerosis 194: 144-152, 2007.
19. Shih CH, Lin LH, Hsu HT, Wang KH, Lai CY, Chen CM and Ko WC: Hesperetin, a selective phosphodiesterase 4 inhibitor, effectively suppresses ovalbumin-induced airway hyperresponsiveness without influencing xylazine/ketamine-induced anesthesia. Evid Based Complement Alternat Med 2012: 472897, 2012.

20. Kumar B, Gupta SK, Srinivasan BP, Nag TC, Srivastava S and Saxena R: Hesperetin ameliorates hyperglycemia induced retinal vasculopathy via anti-angiogenic effects in experimental diabetic rats. Vascul Pharmacol 57: 201-207, 2012.
21. Jin YR, Han XH, Zhang YH, Lee JJ, Lim Y, Kim TJ, Yoo HS and Yun YP: Hesperetin, a bioflavonoid, inhibits rat aortic vascular smooth muscle cells proliferation by arresting cell cycle. J Cell Biochem 104: 1-14, 2008.
22. Orallo F, Alvarez E, Basaran H and Lugnier C: Comparative study of the vasorelaxant activity, superoxide-scavenging ability and cyclic nucleotide phosphodiesterase-inhibitory effects of hesperetin and hesperidin. Naunyn Schmiedebergs Arch Pharmacol 370: 452-463, 2004.
23. Liu L, Xu DM and Cheng YY: Distinct effects of naringenin and hesperetin on nitric oxide production from endothelial cells. J Agric Food Chem 56: 824-829, 2008.
24. Takumi H, Nakamura H, Simizu T, Harada R, Kometani T, Nadamoto T, Mukai R, Murota K, Kawai Y and Terao J: Bioavailability of orally administered water-dispersible hesperetin and its effect on peripheral vasodilatation in human subjects: Implication of endothelial functions of plasma conjugated metabolites. Food Funct 3: 389-398, 2012.
25. Calderone V, Chericoni S, Martinelli C, Testai L, Nardi A, Morelli I, Breschi MC and Martinotti E: Vasorelaxing effects of flavonoids: Investigation on the possible involvement of potassium channels. Naunyn Schmiedebergs Arch Pharmacol 370: 290-298, 2004.
26. Liu Y, Niu L, Cui L, Hou X, Li J, Zhang X and Zhang M: Hesperetin inhibits rat coronary constriction by inhibiting Ca(2+) influx and enhancing voltage-gated K(+) channel currents of the myocytes. Eur J Pharmacol 735: 193-201, 2014.
27. McGrath JC and Lilley E: Implementing guidelines on reporting research using animals (ARRIVE etc.): New requirements for publication in BJP. Br J Pharmacol 172: 3189-3193, 2015.
28. Scholey JW and Meyer TW: Control of glomerular hypertension by insulin administration in diabetic rats. J Clin Invest 83: 1384-1389, 1989.
29. Kanaze FI, Bounartzi MI, Georgarakis M and Niopas I: Pharmacokinetics of the citrus flavanone aglycones hesperetin and naringenin after single oral administration in human subjects. Eur J Clin Nutr 61: 472-477, 2007.
30. Kumar B, Gupta SK, Srinivasan BP, Nag TC, Srivastava S, Saxena R and Jha KA: Hesperetin rescues retinal oxidative stress, neuroinflammation and apoptosis in diabetic rats. Microvasc Res 87: 65-74, 2013.
31. Cogolludo A, Moreno L, Bosca L, Tamargo J and Perez-Vizcaino F: Thromboxane A2-induced inhibition of voltage-gated K+ channels and pulmonary vasoconstriction: Role of protein kinase Czeta. Circ Res 93: 656-663, 2003.
32. Gradel AKJ, Salomonsson M, Sorensen CM, Holstein-Rathlou NH and Jensen LJ: Long-term diet-induced hypertension in rats is associated with reduced expression and function of small artery SKCa, IKCa, and Kir2.1 channels. Clin Sci (Lond) 132: 461-474, 2018.
33. Albarwani S, Nemetz LT, Madden JA, Tobin AA, England SK, Pratt PF and Rusch N: Voltage-Gated K+ channels in rat small cerebral arteries: Molecular identity of the functional channels. J Physiol 551: 751-763, 2003.
34. Shen X, Li H, Li W, Wu X and Ding X: Pioglitazone prevents hyperglycemia induced decrease of AdipoR1 and AdipoR2 in coronary arteries and coronary VSMCs. Mol Cell Endocrinol 363: 27-35, 2012.
35. Livak KJ and Schmittgen TD: Analysis of relative gene expression data using real-time quantitative PCR and the 2(-Delta Delta C(T)) method. Methods 25: 402-408, 2001.
36. Li H, Chai Q, Gutterman DD and Liu Y: Elevated glucose impairs cAMP-mediated dilation by reducing Kv channel activity in rat small coronary smooth muscle cells. Am J Physiol Heart Circ Physiol 285: H1213-H1219, 2003.
37. Dick GM, Bratz IN, Borbouse L, Payne GA, Dincer UD, Knudson JD, Rogers PA and Tune JD: Voltage-Dependent K+ channels regulate the duration of reactive hyperemia in the canine coronary circulation. Am J Physiol Heart Circ Physiol 294: H2371-H2381, 2008.
38. Ohanyan V, Yin L, Bardakjian R, Kolz C, Enrick M, Hakobyan T, Kmetz J, Bratz I, Luli J, Nagane M, *et al*: Requisite role of kv1.5 channels in coronary metabolic dilation. Circ Res 117: 612-621, 2015.
39. Gheibi S, Kashfi K and Ghasemi A: A practical guide for induction of type-2 diabetes in rat: Incorporating a high-fat diet and streptozotocin. Biomed Pharmacother 95: 605-613, 2017.
40. Fang XK, Gao J and Zhu DN: Kaempferol and quercetin isolated from Euonymus alatus improve glucose uptake of 3T3-L1 cells without adipogenesis activity. Life Sci 82: 615-622, 2008.
41. Yang DK and Kang HS: Anti-Diabetic effect of cotreatment with quercetin and resveratrol in streptozotocin-induced diabetic rats. Biomol Ther (Seoul) 26: 130-138, 2018.
42. Wright IK, Amirchetty-Rao S and Kendall DA: Potentiation by forskolin of both SNP- and ANP-stimulated cyclic GMP accumulation in porcine isolated palmar lateral vein. Br J Pharmacol 112: 1146-1150, 1994.
43. Elms SC, Toque HA, Rojas M, Xu Z, Caldwell RW and Caldwell RB: The role of arginase I in diabetes-induced retinal vascular dysfunction in mouse and rat models of diabetes. Diabetologia 56: 654-662, 2013.
44. Mokhtar SS, Vanhoutte PM, Leung SW, Suppian R, Yusof MI and Rasool AH: Reduced nitric oxide-mediated relaxation and endothelial nitric oxide synthase expression in the tail arteries of streptozotocin-induced diabetic rats. Eur J Pharmacol 773: 78-84, 2016.
45. Malakul W, Thirawarapan S, Ingkaninan K and Sawasdee P: Effects of kaempferia parviflora wall. Ex baker on endothelial dysfunction in streptozotocin-induced diabetic rats. J Ethnopharmacol 133: 371-377, 2011.
46. Goulopoulou S, Hannan JL, Matsumoto T, Ogbi S, Ergul A and Webb RC: Reduced vascular responses to soluble guanylyl cyclase but increased sensitivity to sildenafil in female rats with type 2 diabetes. Am J Physiol Heart Circ Physiol 309: H297-H304, 2015.
47. Radovi T, Bömicke T, Kökény G, Arif R, Loganathan S, Kécsán K, Korkmaz S, Barnucz E, Sandner P, Karck M and Szabó G: The phosphodiesterase-5 inhibitor vardenafil improves cardiovascular dysfunction in experimental diabetes mellitus. Br J Pharmacol 156: 909-919, 2009.
48. Wu GB, Zhou EX, Qing DX and Li J: Role of potassium channels in regulation of rat coronary arteriole tone. Eur J Pharmacol 620: 57-62, 2009.
49. Salomonsson M, Brasen JC and Sorensen CM: Role of renal vascular potassium channels in physiology and pathophysiology. Acta Physiol (Oxf) 221: 14-31, 2017.
50. Dick GM and Tune JD: Role of potassium channels in coronary vasodilation. Exp Biol Med (Maywood) 235: 10-22, 2010.
51. Berwick ZC, Moberly SP, Kohr MC, Morrical EB, Kurian MM, Dick GM and Tune JD: Contribution of voltage-dependent K+ and Ca2+ channels to coronary pressure-flow autoregulation. Basic Res Cardiol 107: 264, 2012.
52. Nishijima Y, Cao S, Chabowski DS, Korishettar A, Ge A, Zheng X, Sparapani R, Gutterman DD and Zhang DX: Contribution of KV1.5 channel to hydrogen peroxide-induced human arteriolar dilation and its modulation by coronary artery disease. Circ Res 120: 658-669, 2017.
53. Ohanyan V, Yin L, Bardakjian R, Kolz C, Enrick M, Hakobyan T, Kmetz J, Bratz I, Luli J, Nagane M, *et al*: Requisite role of kv1.5 channels in coronary metabolic dilation. Circul Res 117: 612-621, 2015.
54. Dong Y, Fernandes C, Liu Y, Wu Y, Wu H, Brophy ML, Deng L, Song K, Wen A, and Wong S: Role of endoplasmic reticulum stress signalling in diabetic endothelial dysfunction and atherosclerosis. Diab Vasc Dis Res 14: 14-23, 2017.
55. Kerr PM, Clement-Chomienne O, Thorneloe KS, Chen TT, Ishii K, Sontag DP, Walsh MP and Cole WC: Heteromultimeric Kv1.2-Kv1.5 channels underlie 4-aminopyridine-sensitive delayed rectifier K(+) current of rabbit vascular myocytes. Circ Res 89: 1038-1044, 2001.
56. Thorneloe KS, Chen TT, Kerr PM, Grier EF, Horowitz B, Cole WC and Walsh MP: Molecular composition of 4-aminopyridine-sensitive voltage-gated K(+) channels of vascular smooth muscle. Circ Res 89: 1030-1037, 2001.
57. Nieves-Cintrón M, Syed AU, Nystoriak MA and Navedo MF: Regulation of voltage-gated potassium channels in vascular smooth muscle during hypertension and metabolic disorders. Microcirculation 25, 2018.